GAVIN PUBLISHERS

Archives of Laser and Photonics

Huang JS, et al. Arch Laser Photonics 2: 106.

DOI: 10.29011/ALP-106.100006

Review Article

Electrostatic Discharge for Nano Photonics

Jack Jia-Sheng Huang[1,2*], Deo Yu[2], NiYeh Wu[2], Yu-Heng Jan[2,1], HuiLin Huang[2], Emin Chou[2]

[1]Source Photonics, 8521 Fallbrook Avenue, Suite 200, West Hills, CA 91304, USA

[2]Source Photonics, No. 46, Park Avenue, 2nd Road, Science-Based Industrial Park, Hsinchu, Taiwan

[*]**Corresponding author:** Jack Jia-Sheng Huang, Source Photonics, 8521 Fallbrook Avenue, Suite 200, West Hills, CA 91304, USA, Source Photonics, No. 46, Park Avenue 2nd Road, Science-Based Industrial Park, Hsinchu, Taiwan. Email: jack.huang@sourcephotonics.com

Citation: Huang JS, Yu D, Wu N, Jan YH, Huang H, et al. (2019) Electrostatic Discharge for Nano Photonics. Arch Laser Photonics 2: 106. DOI: 10.29011/ALP-106.100006

Received Date: 09 February, 2019; Accepted Date: 12 March, 2019; Published Date: 20 March, 2019

Abstract:

Electrostatic discharge (ESD) occurs in almost all aspects of our lives. Lightning is an example of ESD that typically occurs during thunderstorms. To prevent building structures from being damaged, lightning rods are often used to preferentially shunt the lightning strike to the ground. ESD can cause damage to modern semiconductor devices as well. For nanoelectronics and nanophotonics, the devices may become more sensitive to ESD due to the smaller feature sizes. To come up with an effective "lightning rod" for nanophotonics, detailed characterization and understanding of ESD-failure mechanisms are critical. In this work, we study the ESD-degradation characteristics of nanoscale short-cavity semiconductor lasers. We perform ESD testing of the lasers over a wide range of stress levels to map out the entire ESD spectrum under the reverse polarity. We show that the lasers exhibit three ESD damage levels: (1) avalanche breakdown, (2) Joule heating, and (3) thermal runaway. We discuss the physical mechanism of each ESD damage level.

Keywords: Electrostatic Discharge; Static Electricity; Semiconductor; Nano Photonics; ESD Damage; Reverse Current; ESD Level

Introduction

Around 585 BC, Thales of Miletus from Greece discovered the principle of static electricity [1]. He observed that amber could attract lightweight objects such as feathers to itself by rubbing the amber with a piece of fur. Today, static Electricity or Electrostatic Discharge (ESD) occurs almost everywhere. Lightning is a vivid example of ESD that occurs during thunderstorms [2]. This discharge allows charged regions in the clouds to temporarily equalize themselves. The principle of the lightning rod was first detailed by Benjamin Franklin in Pennsylvania in 1749. After conducting a kite experiment in a thunderstorm, Franklin invented a lightning rod that consisted of a metal rod mounted on a building structure. The rod was intended to protect the structure from a lightning strike. If lightning hits the structure, it will preferentially strike the rod and be conducted to ground through a wire, instead of passing through the structure and causing fire or electrocution.

To modern man-made devices, ESD also poses similar threat and damage. The ESD failures have been reported in electronic Integrated Circuits (ICs) and optoelectronic devices [3-10]. When devices continue to be miniaturized, the ESD sensitivity is expected to become even more pronounced. Characterization of ESD thresholds and understanding of ESD-failure mechanisms are critical for the development of future Nano electronic and Nano photonic devices [3,7].

In this paper, we study the ESD-degradation characteristics of nanoscale short-cavity semiconductor lasers. We perform ESD testing of the lasers over a wide range of stress voltages (100 - 8000 V) under the reverse polarity. We show that the lasers exhibit three ESD damage levels: (1) avalanche breakdown, (2) Joule heating, and (3) thermal runaway. We discuss the physical mechanism of each ESD damage level.

Experiment

Figure 1(a) shows the schematic of the nanoscale Fabry-Perot (FP) semiconductor laser. To achieve uncooled performance from -40 to +90 °C, nanoscale Multi-Quantum Well (MQW)

and Separate Confinement (SCH) structures of InAlGaAs material were grown by Metal Organic Chemical Vapor Deposition (MOCVD) technique. The thicknesses of the quantum barrier and well in the active region were less than 10 nm. A 20 nm InP layer was then grown to form a Nano-spacer between the active region and the InP cladding layer to minimize current spreading and enhance bandwidth. The final InP cladding layer and a heavily-doped p^+-InGaAs layer were grown and etched to form a 1.5 µm wide ridge waveguide (RWG) structure. Finally, the p-metal of Ti/Pt/Au was deposited and annealed to make an Ohmic contact. The wafer was thinned and deposited with n-metal of AuGe/TiAu [11-13]. The wafers were cleaved into 150 µm long bars to form short-cavity lasers for 25 Gb/s high-speed applications. The laser facets were deposited with anti-reflection (AR) and highly-reflective (HR) coatings. The reflectivity of the AR coating was 50%. The laser chips were mounted to the submount package and stressed with different levels of ESD.

Figure 1(b) shows the ESD test setup with a human-body model (HBM) simulator consisting of a circuit of 1.5 kΩ and 100 pF. The HBM test method was in adherence to Telcordia TR-NWT-000870 [14]. The chip-on-sub mount device was loaded to a test station, and the probes made contacts to the bond pads of the surmounts that were connected to the p-side and n-sides of the laser device. The ground of the ESD tester was connected to the n-side (cathode) of the laser, whereas the ESD pulse was applied to the p-side (anode) of the laser. The ESD stress voltage started from 0.1 kV and ramped successively up to 8 kV in order to observe the entire evolution of ESD failure morphology. Current versus voltage (IV) was measured before and after each ESD stress to determine the ESD-failure threshold [11]. The ESD failure was defined as a reverse voltage change of over 1 V at the reverse current of 1 µA. After an ESD failure, the devices were randomly selected for Failure Analysis (FA). Optical microscopy and Scanning Electron Microscopy (SEM) were used for the physical FA.

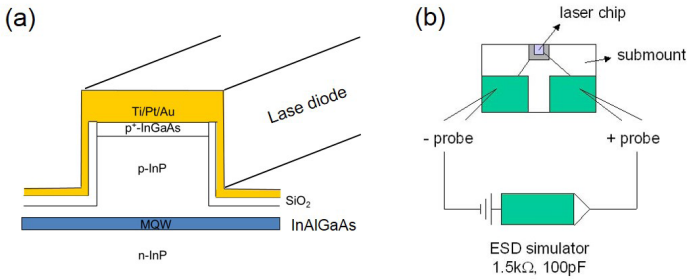

Figure 1: Schematic of (a) nanoscale InAlGaAs MQW laser structure and (b) laser chip on sub mount for ESD test.

Results and Discussions

For the short-cavity laser with a cavity length of 150 µm and a ridge width of 1.5 µm, the device is subjected to a high electric field during the ESD stress, as illustrated in Figure 2. The majority of the high electric field is concentrated in the MQW active region with minimal leakage to the lateral directions. The small lateral leakage is mainly due to the Nano-spacer that is formed to minimize current spreading for performance optimization. This applies to both forward and reverse ESD stresses.

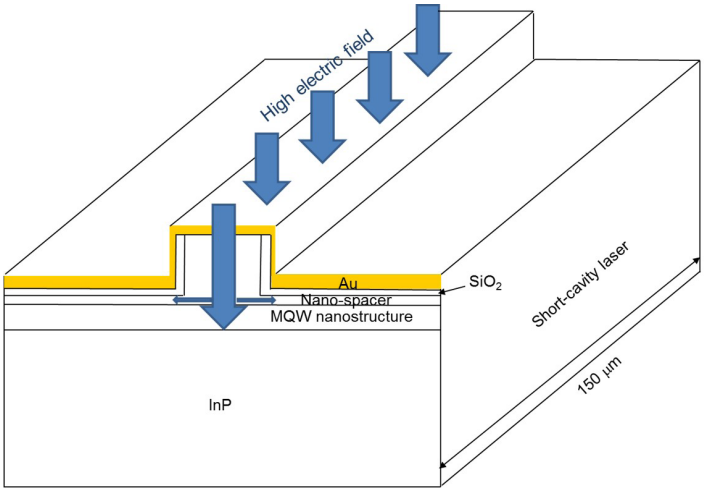

Figure 2: Schematic of short-cavity laser under ESD stress (not in scale). The laser experiences high electric field in the MQW active region with minimal leakage to the lateral directions.

The typical IV curve of the 150 µm long InAlGaAs MQW laser is shown in Figure 3. The turn-on voltage at 25 °C was approximately 0.9 V. Above the turn-on voltage, the forward current increased rapidly with increasing voltage. In this regime, the series resistance (R_s) can be extracted from the slope of IV curve.

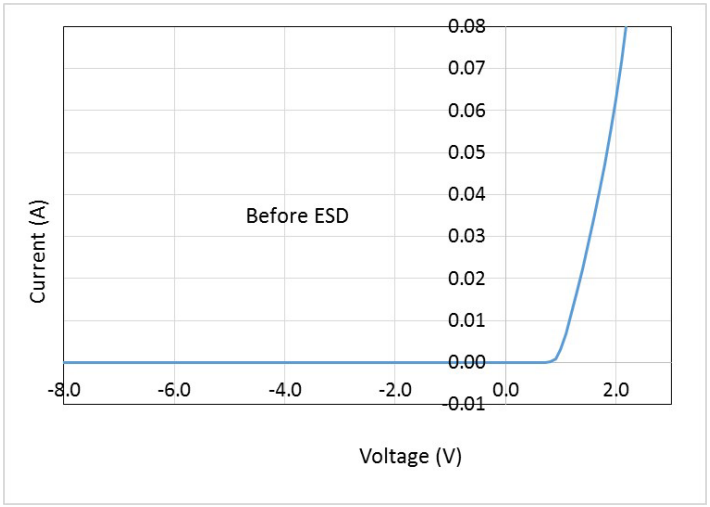

Figure 3: A typical IV characteristic of 150 µm long InAlGaAs MQW laser. The IV is measured in forward and reverse polarities at 25 °C.

Figure 4 shows the IV curves before and after different degrees of ESD stresses. As the reverse ESD stress ramped up to -600 V, the reverse IV started to show a small shift. At the initial ESD degradation, the chip normally did not exhibit any physical damage to the surface. As the reverse ESD stress increased to -1200 V, the IV started to show more substantial changes in both forward and reverse polarities. For the forward IV, the turn-on voltage decreased, indicating that the junction had been damaged. For the reverse IV, the leakage current grew larger at the fixed voltage. While the IV change in ESD level-2 was significant, the chip typically did not show any visible surface damage. To compile the entire ESD degradation process, the laser was ESD stressed up to -8000 V.

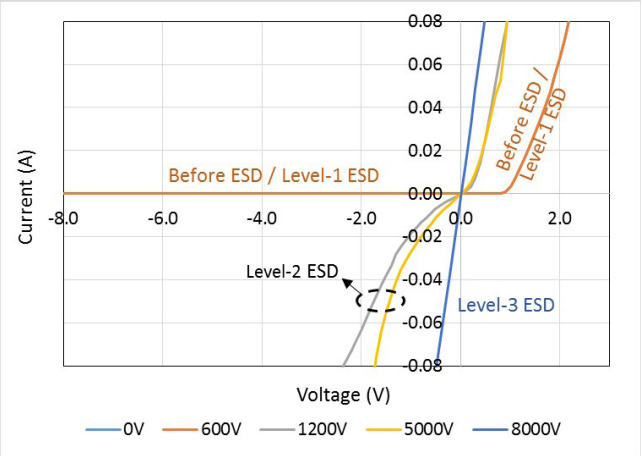

Figure 4: Typical IV curves of 150 µm long InAlGaAs MQW lasers before and after various ESD stresses. Level-1, Level-2 and Level-3 ESDs are denoted to indicate different levels of ESD damages.

In the following, we discuss each ESD damage level by means of electrical and physical characterizations.

Level-1: Avalanche breakdown

Level-1 ESD degradation is characterized by a small shift in reverse IV. At this early ESD stage, the degradation of reverse ESD is largely driven by avalanche breakdown resulting from the tunneling mechanism [15]. Avalanche breakdown occurs when an excessive electric field forms in the semiconductor during the reverse ESD stress [3]. The high electric field accelerates electrons and holes to sufficient energy to knock other electrons and holes free. The field accelerates these additional electron and hole carriers that can generate more electron-hole pairs in a growing snowball process called avalanche breakdown.

The shift of Level-1 ESD is so small that it usually cannot be deciphered from the linear scale. For example, the IV curves before the ESD stress appears to overlap with that of the Level-1 ESD in Figure 4. To discern the subtle difference in the reverse IV at Level-1 ESD, a logarithmic scale is typically expressed as shown in Figure 5. In the log scale, it can be seen that the reverse current becomes larger after Level-1 ESD degradation. For instance, the reverse current increases by roughly 1 order of magnitude of the reverse voltage of -2 V.

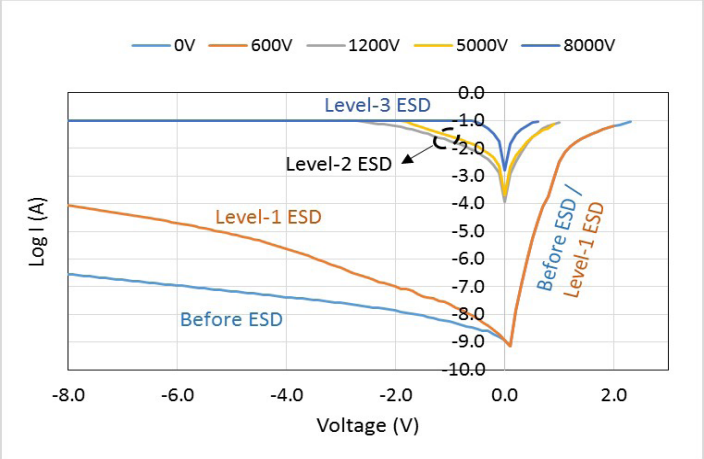

Figure 5: Log scale of IV curves of 150 µm long InAlGaAs MQW lasers before and after various ESD stresses. Level-1, Level-2 and Level-3 ESDs are denoted to indicate different degrees of ESD damages.

Level-2: Joule heating

Level-2 ESD degradation is featured with substantial change in both forward and reverse IV. The IV shift is significant enough to be observed in both linear and logarithmic scales of IV curves. For the forward IV, the turn-on voltage becomes smaller, indicating that the p-n junction had degraded. In the reverse direction, the reverse current, typically increases by several orders of magnitude as the reverse voltage of -2 V as shown in Figure 5.

At Level-2 ESD, the device degradation is attributed to avalanche breakdown and Joule heating. The thermal heating may accelerate the reverse breakdown process. The ESD damage at this level may not be catastrophic, so it cannot be manifested on the chip surface as shown in Figure 6.

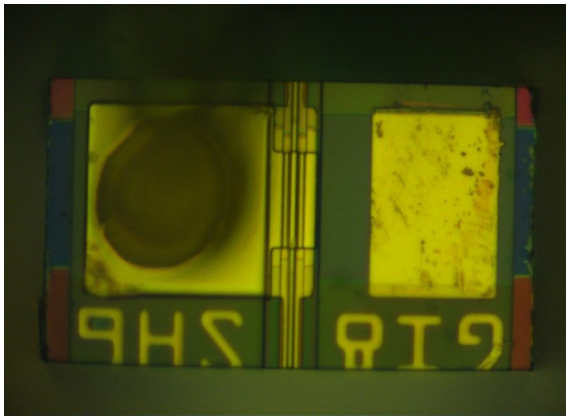

Figure 6: Top view of 150 µm long InAlGaAs MQW laser after being subjected to reverse ESD stress of -1200 V. The damage corresponds to Level-2 ESD according to the IV curve

Level-3: Thermal runaway

As the reverse ESD voltage continues to increase, thermal runaway process eventually occurs at Level-3 ESD. At the location of current crowding, more current tends to flow through the hot region. Subsequently, the resistance of the hot region decreases with the rising temperature. This in turn attracts more current to flow into the hot region and exacerbates the heating. The current concentration and heat-induced resistance reduction forms a positive loop to cause thermal runaway.

Figure 7 shows the example of the damaged laser line after the reverse ESD stress at -6000 V. In the hot region shown by thermal emission microscopy (EMMI), damage can be visually seen on the laser line near the edge of bond pad.

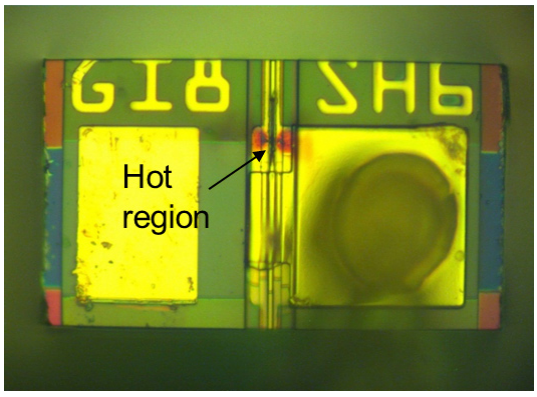

Figure 7: Top view of 150 µm long InAlGaAs MQW laser after being subjected to reverse ESD stress of -6000 V. The damage corresponds to Level-3 ESD according to the IV curve.

Conclusion

We have extensively studied the reverse ESD characteristics of nanoscale short-cavity FP semiconductor lasers over a wide range of ESD levels. Based on the electrical and physical properties, the ESD is categorized into three degradation levels. The first ESD degradation level is driven by avalanche breakdown. Only the reverse IV shows a small shift that can be deciphered in logarithmic scale. The forward IV remains intact, and no surface damage occurs at Leve-1 ESD. The ESD degradation of Level-2 is accelerated by Joule heating. The IV shift is significant enough to be observed in both linear and logarithmic scales of IV curves. For the forward IV, the turn-on voltage becomes smaller, indicating that the p-n junction has been degraded. For the reverse direction, the reverse current, typically increases by several orders of magnitude of the reverse voltage of -2 V. The ESD damage at Level-2 may not be catastrophic and manifested on the chip surface. At Level-3 ESD, the damage is catastrophic, and visible damage can be seen on the surface of the chip. The burn mark can be observed in the laser line near the bond pad. Thermal runaway plays very important role in the catastrophic ESD damage. At the location of current crowding, more current flows through the hot region during Level-3 ESD. Subsequently, the resistance of the hot region decreases with the rising temperature. This in turn attracts more current to flow into the hot region and exacerbates the heating, leading to thermal runaway.

References

1. https://en.wikipedia.org/wiki/Thales_of_Miletus
2. https://en.wikipedia.org/wiki/Lightning
3. Voldman SH (2002) Lightning rods for Nano-electronics. Sci American 91-97.
4. Twu Y, Cheng LS, Chu SNG, Nash FR, Wang KW, et al. (1993) Semiconductor laser damage due to human-body-model electrostatic discharge. J Appl Phys 74: 1510-1520.
5. Jeong J, Park KH, Park HM (1995) Wavelength shifts of 1.5 µm DFB lasers due to human-body model electrostatic discharge followed by accelerated aging experiments. J Lightw Technol 13: 186-190.
6. DeChiaro LF, Sandroff CJ (1992) Improvements in electrostatic discharge performance of InGaAsP semiconductor lasers by facet passivation. IEEE Trans Electron Devices 39: 561-565.
7. Huang JS, Olson T, Isip E (2007) Human-body-model electrostatic discharge and electrical overstress studies of buried hetero-structure semiconductor lasers. IEEE Trans Device Materials Reliability 7: 453-461.
8. Huang JS, Lu H (2009) Size effect on ESD threshold and breakdown behavior of InP buried hetero structure semiconductor lasers. Open Appl Phys J 2: 5-10.
9. Sim SP, Robertson MJ, Plumb RG (1984) Catastrophic and latent damage in GaAlAs lasers caused by electrical transients. J Appl Phys 55: 3950-3955.
10. Ichikawa H, Kumagai A, Kono N, Matsukawa S, Fukuda C, et al. (2010) Dependence of facet stress on reliability of AlGaInAs edge-emitting lasers. Appl Phys 107.

11. Huang JS, Jan YH, Chang R, Klotzkin D, Shyu C, et al. (2016) Design-in ESD reliability of 10 Gb/s uncooled (-40 to +85 °C), harsh-environmental lasers for 4G wireless mobile networks. IEEE AVFOP, USA.

12. Huang JS, Jan YH, Chang R, Shiu G, Chou E (2018) Front-rear LI linearity correlation of InGaAlAs uncooled (-40 °C to +90 °C) DML for robust tracking error in 10G-EPON ONU. CLEO Pacific Rim Conference, USA.

13. Huang JS, Miao RS, Lu H, Helms C, Wang C, et al. (2007) Theoretical and experimental thermal analysis of InP ridge lasers on sub mounts and TO packages. IEEE Transactions Device and Materials Reliability 7: 363-368.

14. (1991) Electrostatic Discharge Control in the Manufacture of Telecommunications Equipment.

15. Huang JS (2015) Reliability of Optoelectronics. Reliability Characterization of Electrical and Electronic Systems 83-114.